Proc. Natl. Acad. Sci. USA
Vol. 86, pp. 1826–1830, March 1989
Biochemistry

Biological photocathodes

(photoelectron microscopy/charge transfer/cesium/heme/chlorophyll-rich thylakoid membranes)

O. HAYES GRIFFITH, DOUGLAS L. HABLISTON, G. BRUCE BIRRELL, WALTER P. SKOCZYLAS, AND KAREN K. HEDBERG

Institute of Molecular Biology, University of Oregon, Eugene, OR 97403

Communicated by Peter H. von Hippel, December 16, 1988

ABSTRACT **Biological surfaces emit electrons when subjected to UV light. This emission is increased greatly after exposure to cesium vapor. Increases from 2 to 3 orders of magnitude are observed, depending on the biochemicals present. Heme and chlorophyll exhibit unusually high photoemission currents, which are increased further after cesiation. Photoemission from proteins and lipids is much less but also is increased by exposure to cesium. The formation of photocathodes with cesium greatly increases the practical magnifications attainable in photoelectron microscopy of organic and biological specimens. Photoelectron micrographs taken at magnifications ≥ ×100,000 of chlorophyll-rich thylakoid membranes and of colloidal gold-labeled cytoskeleton preparations of cultured epithelial cells demonstrate the improvement in magnification. The selectivity and stability of the photocathodes suggest the possibility of detecting chromophore binding proteins in membranes and the design of photoelectron labels for tagging specific sites on biological surfaces.**

The photoelectric effect explained in the epoch paper of Einstein in 1905 has contributed much information in the physical sciences but has yet to have a corresponding impact on the biological sciences. To derive information from the photoelectric effect, the biological surface must become the photocathode, emitting electrons excited by UV light. The electrons can then be accelerated and imaged in a photoelectron microscope (1), as diagrammed in Fig. 1, or analyzed by spectroscopy. The information content is potentially high, since molecules differ in their ionization potentials, and this provides a probe of molecular structure. In addition, the photoelectron image is sensitive to fine surface detail. The optical analog is fluorescence microscopy, which is already widely used in cell biology. Photoelectron microscopy has the advantage of a much higher theoretical resolving power than that of fluorescence microscopy because the emitted electrons have much shorter wavelengths than emitted (fluorescent) light. However, an obstacle in photoelectron imaging is the low emissivity of biological surfaces, which limits the effective magnification. The challenge is to convert the biological surface into a sensitive photocathode while retaining the differences in photoemissivities of key components (e.g., chromophores or labeled sites).

Hints on how to increase the image brightness can be found in early studies aimed at improving the sensitivity of alkali metal cathodes. In the 1930s, for example, Oplin (2) and Suhrmann and coworkers (3, 4) noted changes in the photoelectric emission of sodium, potassium, and cesium surfaces after treatment of a variety of chemicals including organic dyes and aromatic hydrocarbons. In the 1960s, Setton and Bazin (5) examined the photoelectric behavior of cesium-treated graphite, Inokuchi and Harada and coworkers (6, 7) reported high quantum yields from surfaces of cesium combined with polycyclic aromatic compounds, and Marchetti and Kearns (8) measured the photoelectric yield and absorption spectra of thin films of potassium combined with anthracene and with perylene. Also relevant is the work of Aleksandrov and Belkind (9, 10) on the lowering of the work function of thin films of aromatic hydrocarbons by sodium and cesium. Although there are considerable differences in results owing to the difficulty in working with clean surfaces of alkali metals, these studies indicate that certain types of

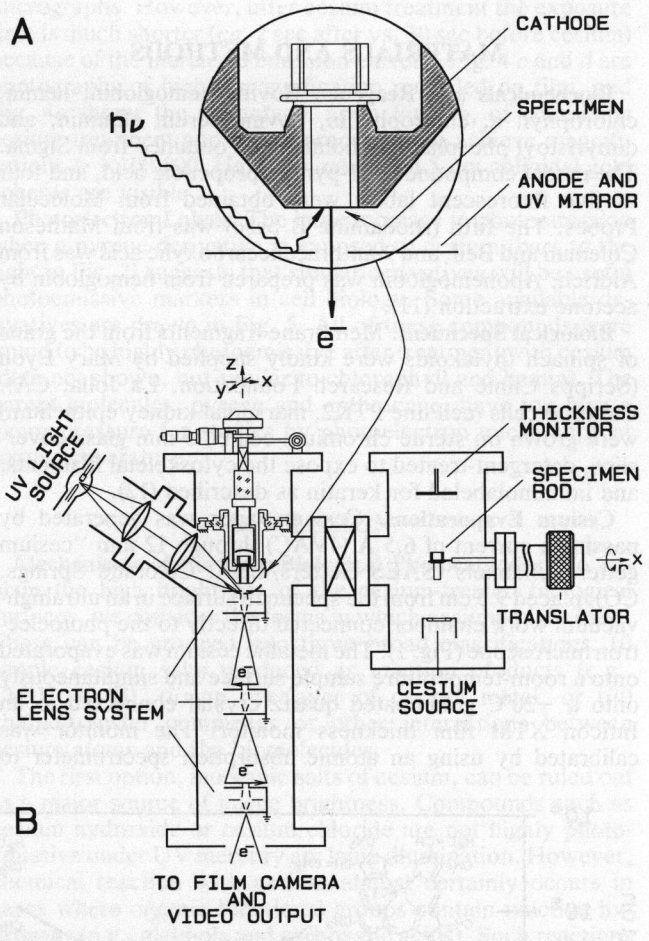

FIG. 1. (*A*) The photoemission process, as it occurs in a photoelectron microscope. UV light ($h\nu$) causes the photoemission of electrons (e^-) from the specimen surface. The electrons are accelerated across the cathode–anode gap before entering the electron lens system. (*B*) Simplified diagram of the photoelectron microscope and the work chamber constructed for these experiments. After evacuation and exposure to cesium metal vapor, the specimens are translated into the microscope. The accelerated photoelectrons are imaged by objective, intermediate, and projector lenses similar to those of a transmission microscope. The image is then recorded on film or an image intensifier/TV system.

The publication costs of this article were defrayed in part by page charge payment. This article must therefore be hereby marked "*advertisement*" in accordance with 18 U.S.C. §1734 solely to indicate this fact.

organic molecules form stable photoemissive complexes with cesium, rather than simply reacting with the metal.

In this paper we report the photoemissive properties of biological surfaces after exposure to cesium metal vapor. Stable photocathodes are formed with the important prosthetic groups heme and chlorophyll. Cesium enhances the photoemission of most biological macromolecules, largely overcoming the obstacle that heretofore had limited the magnifications possible in photoelectron micrographs of biological surfaces. During the course of this work, some fluorescent probes were identified that, when combined with cesium, also can form photoemissive labels for the identification of specific sites.

MATERIALS AND METHODS

Biochemicals and Reagents. Bovine hemoglobin, hemin, chlorophyll a, chlorophyllin, bovine serum albumin, and dimyristoyl phosphatidylcholine were obtained from Sigma. The model compound, 3-(1-pyrene)propenoic acid, and four of five fluorescent labels were obtained from Molecular Probes. The fifth (rhodamine B base) was from Matheson Coleman and Bell, and 9-anthracenecarboxylic acid was from Aldrich. Apohemoglobin was prepared from hemoglobin by acetone extraction (11).

Biological Specimens. Membrane fragments from the grana of spinach thylakoids were kindly supplied by Mary Lyon (Scripps Clinic and Research Foundation, La Jolla, CA). Cultured cells (cell line PTK2, marsupial kidney epithelium) were grown on sterile chromium-coated 5-mm glass coverslips, detergent-treated to expose the cytoskeletal filaments, and immunolabeled for keratin as described (12).

Cesium Evaporations. Cesium vapor was generated by passing a current of 6.5 A (4VAC) through 12-mm "cesium getter" channels (SAES Getters/USA, Colorado Springs, CO), placed 9.5 cm from the specimen surface in an ultrahigh-vacuum work chamber connected directly to the photoelectron microscope (Fig. 1). The metallic cesium was evaporated onto a room-temperature sample surface and simultaneously onto a −20°C gold-coated quartz crystal connected to an Inficon XTM film thickness monitor. The monitor was calibrated by using an atomic absorption spectrometer to measure the amount of cesium washed from a glass plate mounted at the sample plane. Routinely, 1 nm of cesium was evaporated onto specimens monitored in this fashion before introduction into the photoelectron microscope.

Photoelectron Microscopy and Beam Current Measurements. The photoelectron microscope is an oil-free ultrahigh vacuum instrument designed for minimum contamination of the specimen surfaces (1). Both the photoelectron emission (beam currents) and micrographs were obtained with this instrument by using UV light from a short-arc mercury lamp (Osram HBO 100). For beam-current measurements, duplicate samples were prepared by either vacuum sublimation or solvent deposition of the chemicals onto 5-mm chromium-coated glass coverslips. The induced beam current was measured with a Keithley 26000 picoammeter interfaced to a Dascon-1 A/D data acquisition card in an IBM RT computer. For photoelectron microscopy, the images were recorded either on electron image film or on a phosphor fiber optically coupled to an image intensifier and video camera. The video signal was digitized and stored with an Image Technology/G. W. Hannaway image-processing system coupled to an IBM RT computer and a Dunn Instruments image recorder.

RESULTS

Photoelectron Emission of Biological Molecules. Cesium interactions with biological molecules were examined by exposing thin films to cesium vapor and measuring the resulting changes in photoelectron emission. These measurements indicate substantial increases in electron emission from biological molecules after cesium treatment, as shown in the semilogarithmic plot of Fig. 2. The photocathodes were quite stable. The photoelectric behavior remained very nearly constant over a period of hours in the photoelectron microscope. As expected, when taken out of the vacuum chamber, the photocathodes were quickly destroyed, presumably by atmospheric oxygen and water vapor.

There are large differences in the photoelectron currents, depending on the structure of the biomolecules. For example, the first three bars of Fig. 2 are for hemoglobin and its two components, the polypeptides (apohemoglobin) and the heme group (hemin). Even without cesium, the photoemission of hemin is about 2 orders of magnitude greater than for apohemoglobin and accounts for much of the emission from the intact hemoglobin (Fig. 2 and ref. 1). After exposure to cesium vapor, there is a large increase in all three emission currents, as shown in Fig. 2, but the ratios remain in the same order, with hemin the highest. Like hemin, chlorophyll a and a derivative, chlorophyllin, are unusually photoemissive after exposure to cesium, suggesting specific complex formation.

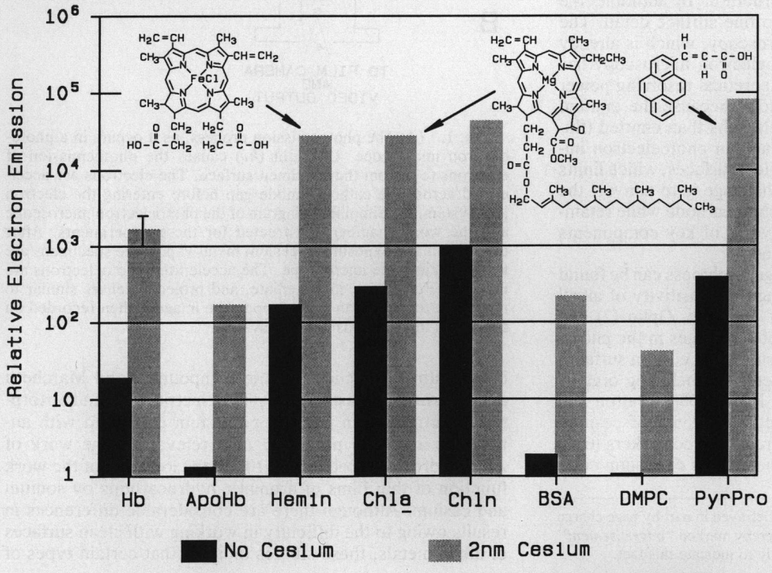

FIG. 2. Biological molecules exhibit greatly enhanced photoemission when exposed to cesium vapor. The bar graph compares the logarithm of the relative electron emission in arbitrary units observed before (dark bars) and after (light bars) coating with a thin layer of cesium. Compounds: Hb, hemoglobin; ApoHb, apohemoglobin; Chla, chlorophyll a; Chln, chlorophyllin; BSA, bovine serum albumin; DMPC, dimyristoyl phosphatidylcholine; PyrPro, a model aromatic compound (a derivative of pyrene): = 3-(1-pyrene)propenoic acid. A second model compound, 9-anthracenecarboxylic acid, exhibited a similar enhancement after exposure to cesium.

Photoelectron Microscopy. Exposure to cesium vapor enhances the photoemission of biological specimens, permitting much higher magnifications than heretofore possible in photoelectron microscopy of biological specimens (Figs. 3 and 4). Cesium, of course, has been used frequently to enhance the brightness of metals and to make semiconductor photocathodes such as cesium antimonide (13). Cesium antimonide has been used (14) to coat the surfaces of optical components so they may be viewed by photoelectron microscopy. We were unable to locate any studies in the literature involving photoelectron microscopy of organic or biological surfaces exposed to cesium.

Fig. 3 is of fragments from thylakoid membranes often called BBY preparations, after the authors (15). These membranes are rich in chlorophyll and are in fact visibly green. No efforts have been made to identify detail in the micrographs or to achieve maximum specimen preservation, since the primary aim here is to assess the effects of cesium on image brightness of untreated specimens. The photoelectron image of the membrane after cesium treatment at a magnification of ×4200 (Fig. 3*a*) required approximately a 30-sec film exposure. Without cesium, the image could not be detected at this magnification. Fig. 3*b* shows the combined results obtained with cesium and an image processor. The magnification is ×158,400. The collection time is 1/30 sec per video frame (1/60 sec for two interlaced images). The final image is a running average of >256 frames; thus, the total collection time is about 9 sec.

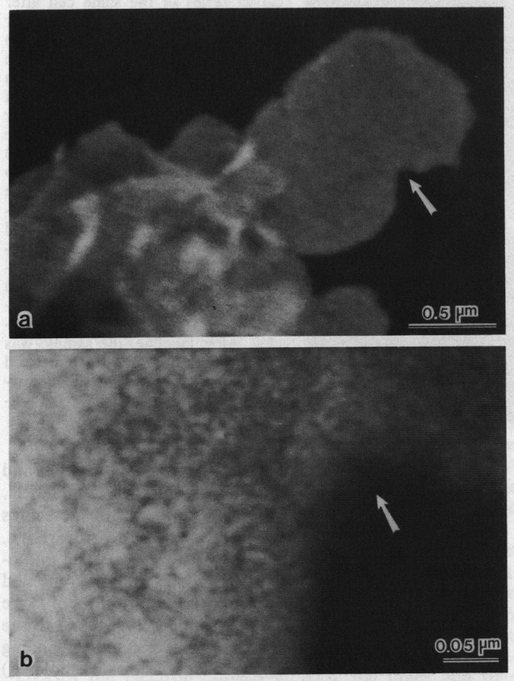

FIG. 3. Cesium treatment of membrane fragments from spinach chloroplasts results in unusually photoemissive samples, making possible high-magnification photoelectron micrographs. (*a*) ×4200. (*b*) ×158,400. The arrow identifies the same location in both micrographs. The specimen, kindly provided by Mary Lyon, was air-dried without fixation to avoid possible chemical effects on specimen brightness.

Fig. 4 is a photoelectron image of a colloidal gold-labeled specimen, typical of that encountered in immunoelectron microscopy studies of cytoskeletal preparations of cultured cells. Fig. 4 *a* and *b* were taken at a low magnification to facilitate comparison of images before and after cesium treatment. The images are similar, indicating that cesium does not cause major problems in the interpretation of micrographs. However, after cesium treatment the exposure time is much shorter (*ca.* 2 sec after vs. 30 sec before cesium) because of the increased emission current. Fig. 4 *c* and *d* are photographs of higher magnification recorded on film, and Fig. 4*e* shows the advantage, as in Fig. 3*b*, of combining cesium treatment and image processing to achieve magnifications > ×100,000. Here the individual 5-nm colloidal gold spheres are visible.

Photoelectron Labels. The large increase in photoemission when a pyrene derivative is exposed to cesium (bars to the right in Fig. 2) suggests that similar derivatives will be useful photoemissive markers in cell biology. Some available derivatives are drawn in Fig. 5. All of these compounds were found to be highly photoemissive after treatment with cesium (data not shown, but similar to chlorophyll and hemin). The parent molecules, pyrene and anthracene, have too high a vapor pressure for studies by photoelectron microscopy at room temperature.

DISCUSSION

Mechanisms of Forming Biological Photocathodes. To explain the high brightness of the cesium-treated biological surfaces, we consider the forms in which cesium might exist. These can be grouped into three broad classifications: (*i*) simple cesium salts produced as reaction products (e.g., CsOH, CsCl), (*ii*) an overlayer of cesium metal, or (*iii*) charge-transfer complexes or other interactions between cesium atoms and the biomolecules.

The first option, inorganic salts of cesium, can be ruled out as a major source of image brightness. Compounds such as cesium hydroxide or cesium chloride are not highly photoemissive under UV mercury arc lamp illumination. However, chemical reaction with cesium almost certainly occurs in cases where organic functional groups contain reactive hydrogens (e.g., alcohols and carboxylic acids). Such reactions can contribute to image contrast by making these sites darker in the photoelectron micrographs.

The second possibility, a uniform overlayer of cesium metal, would result in a bright image. However, it cannot account for the interesting variations in photoemission observed (e.g., Fig. 2). Also, the initial layer of cesium in the present experiments is small, on the order of 1 nm. The vapor pressure of cesium is relatively high at room temperature so that any free cesium metal evaporates, particularly under the action of UV light in the ultrahigh-vacuum photoelectron microscope. For example, it was necessary to cool the quartz crystal of the thickness monitor because cesium was found to evaporate from the surface at room temperature, and this was without illumination. Although there is always the possibility of small residual islands or atoms of cesium, we conclude that a simple uniform metal coating does not explain the experimental results.

The third possibility is almost certainly the correct explanation. However, interactions with biomolecules at the surface can involve several mechanisms because cesium comes in contact with many different exposed functional

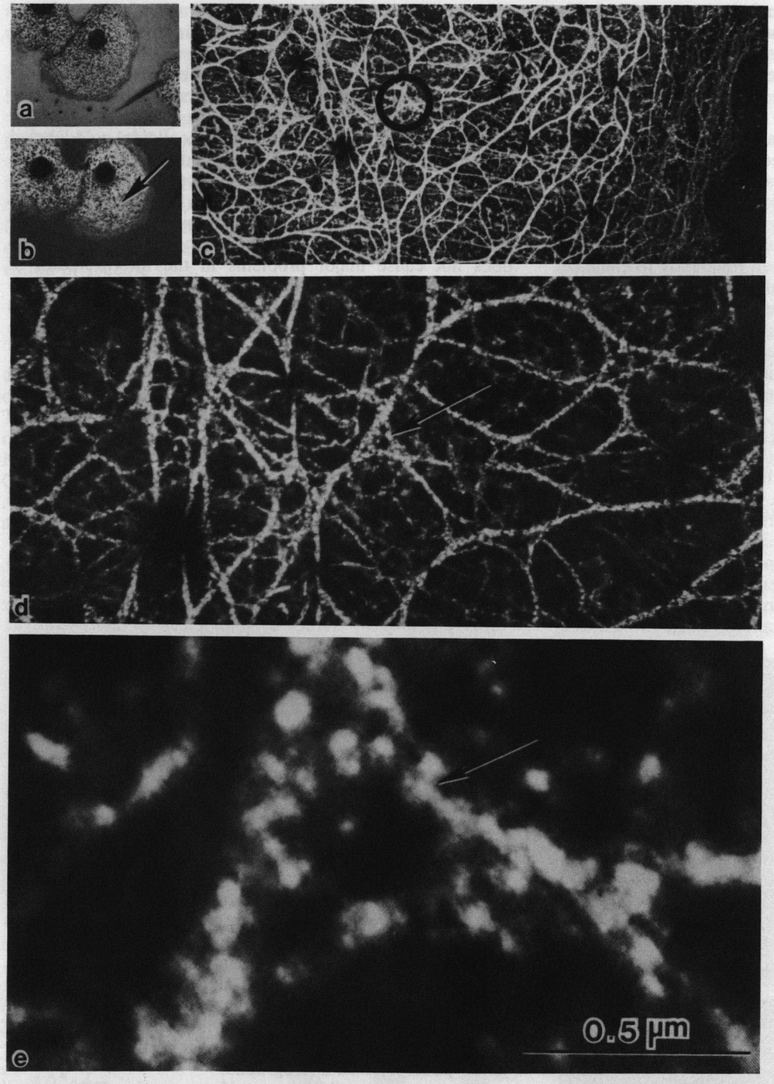

FIG. 4. Zoom series illustrating the high magnifications achievable after cesium treatment of colloidal gold-labeled intermediate filaments of cultured cells. (*a*) Photoelectron micrograph of the preparation before exposure to cesium. (*b–e*) A magnification series of the same cell after evaporation of a very thin (1 nm) layer of cesium metal. (*a* and *b*) ×300; (*c*) ×3050; (*d*) ×10,150; (*e*) ×80,000. The arrows in *b*, *d*, and *e* and the circle in *c* indicate one of the labeled filament bundles that is common to all four micrographs. The cells (cell line PTK2, marsupial kidney epithelium) were first treated with detergent to expose the cytoskeleton, and then the keratin-containing intermediate filaments were labeled with colloidal gold in a two-step procedure: (*i*) treatment with monoclonal antibody recognizing keratin, followed by (*ii*) treatment with a second antibody attached to 5-nm colloidal gold particles. After labeling, the sample was fixed with glutaraldehyde, postfixed with osmium tetroxide, with dehydrated ethanol, and dried at the critical point.

groups in biological specimens. The situation is reminiscent of the interaction of alkali metals with liquid ammonia and amines. As has been known for over a century, alkali metals dissolve in liquid ammonia (16). The alkali metal dissociates, yielding predominantly metal cations, and solvated electrons in dilute solution. In concentrated solutions more complex interactions occur, including ion pairs and higher aggregates, which have yet to be fully characterized. Crown ethers, cryptands, and related organic complexing agents increase the solubility of alkali metals in amine and ether solvents by forming strong complexes with the metal cations (17, 18). Many biological compounds of interest contain amines, suggesting some related, probably weaker, interactions may occur here. Strong interactions can occur between alkali metals and aromatic hydrocarbons yielding charge-transfer complexes (e.g., ion-radical salts). We focus on these complexes because of their potential use in visualizing naturally occurring chromophores such as hemes and chlorophylls and because they provide a way to design photoelectron labels.

Ionization potentials are normally reported for molecules in the gas phase (I_g), and for large aromatic hydrocarbons, they are typically in the range of 7–10 eV (19). The photoelectric behavior of the two model compounds, pyrene and anthracene, is very similar. The experimental values of I_g are 7.5 eV and 7.4 eV, respectively (19), and correspond to the removal of one electron from the highest occupied bonding orbital. The ionization energy (photoemission threshold, I_s) of the corresponding solid aromatic compounds is lower by about 1.5 eV due to polarization effects. Specifically, for surfaces of pure anthracene and pyrene, I_s values are 5.6 eV and 5.8 eV, respectively (20). Solid surfaces of protoporphyrin and chlorophyll are reported to have an I_s of about 5 eV (21, 22). For comparison, the short wavelength limit of the mercury short-arc lamp is about 4.9 eV (254 nm). Thus, the

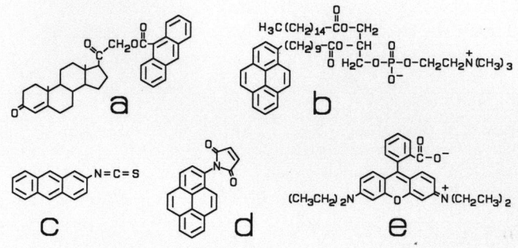

FIG. 5. Representative photoelectron labels. These molecules form highly photoemissive labels when exposed to cesium vapor. The upper two are fluorescent lipid labels: 21-(9-anthroyloxy)-deoxycorticosterone (*a*) and 3-palmitoyl-2-(1-pyrenedecanoyl)-L-α-phosphatidylcholine (*b*). The lower three are fluorescent protein labels: 2-anthraceneisothiocyanate (*c*), *N*-(1-pyrene)maleimide (*d*), and rhodamine B base (*e*), a model for rhodamine-derived covalent labeling reagents.

thresholds of photoemission of these aromatic compounds are almost inaccessible with mercury short-arc illumination, one reason why the photoelectron emission is low before treatment with cesium.

Cesium lowers the effective ionization threshold of these aromatic compounds (**R**) by donating the lone electron from its 6s orbital to the lowest unoccupied orbital of the π-electron system, forming a charge-transfer complex, as illustrated below.

$$Cs + \mathbf{R} \rightleftarrows Cs^+ \mathbf{R}^-$$

Formation of complexes or ion-radical salts between alkali metals and aromatic compounds, producing the negative ion or aromatic hydrocarbons such as pyrene and anthracene, is well documented by electron spin resonance spectroscopy and other techniques (23–25). We were unable to locate any photoelectric studies of alkali metal complexes of chlorophyll and hemes. However, the negative ions of chlorophyll and other porphyrins are known (26, 27). Qualitatively, the reason the ionization energy of aromatic hydrocarbons is lowered is that the unpaired electron now occupies an antibonding orbital and requires less energy to remove by photoionization compared with removal of an electron from a bonding orbital of the parent molecule.

Thus, the principal effect of cesium is to shift the quantum yield curve of the aromatic molecule to longer wavelengths, causing a dramatic increase in photoemission. The essential criterion in this mechanism is the ability of the aromatic molecule to act as an electron acceptor, forming a stable radical anion. Other mechanisms are possible, such as a model involving electron transfer from cesium to shallow traps on the surface (i.e., resembling solvated electrons). A trapped electron model may be useful in accounting for the increased emission of biomolecules such as proteins and lipids that do not have conjugated chromophores.

Photoelectron Micrographs. The impetus for carrying out this study was to enhance image brightness. Brightness, rather than resolution, has usually been the limiting factor in photoelectron microscopy. As with all microscopes, every 10-fold increase in magnification requires a 100-fold increase in the signal-to-noise ratio. Exposure to cesium vapor increases the electron current at least 100 times and thus provides a 10-fold improvement in magnification. Further gains are being made with image processing. The photoelectron micrographs presented here are the first obtained at or above ×100,000. We conclude that cesium treatment in combination with an image processor removes a barrier to the application of photoelectron microscopy in cell biology by making the images sufficiently bright to photograph at high magnifications. Even higher magnifications are possible but will necessitate improvements in the microscope resolution (currently about 10 nm) as well as in the image detectors.

Biological molecules are not equally photoemissive after exposure to cesium. Hemes, chlorophylls, and other large π-conjugated molecules form photocathodes that are nearly 100 times more photoemissive than cesiated proteins and lipids (Fig. 2). This raises the possibility of using the naturally occurring hemes and chlorophylls to image energy-transducing membrane structures in mitochondria and chloroplasts once the instrumental resolution has been improved. Detecting hemes (or chlorophylls) by conventional electron microscopy has not been successful, presumably because electron-scattering cross sections of heme proteins are not sufficiently different from those of nonheme proteins.

Finally, the results on colloidal gold-labeled cytoskeletons indicate that colloidal gold becomes sufficiently more photoemissive after cesium treatment to make it easily detectable as a label at high magnifications. Other markers can be made from pyrene, anthracene (e.g., Fig. 5), and related aromatic hydrocarbons attached to exposed sites on biological structures because pyrene-like conjugated molecules form photoemissive complexes with cesium. Many of the aromatic labels are fluorescent, making possible double-labeling experiments by fluorescence microscopy and photoelectron microscopy.

We are pleased to acknowledge E. Relder and G. Stowe of Varo, Inc., for help and advice with cesium evaporations and to Dr. Mary Lyon for membrane fragments from spinach thylakoids. We also thank Drs. A. Belkind, J. Fajer, Y. Harada, G. F. Rempfer, A. H. Sommer, and S. I. Weissman for useful discussions. This work was supported by Grant CA11695 from the National Cancer Institute and a grant from the M. J. Murdock Charitable Trust.

1. Griffith, O. H. & Rempfer, G. F. (1987) in *Advances in Optical and Electron Microscopy*, eds. Barer, R. & Cosslett, V. E. (Academic, London), Vol. 10, 269–337.
2. Oplin, A. R. (1930) *Phys. Rev.* **36,** 251–259.
3. Suhrmann, R. & Dempster, D. (1935) *Z. Phys.* **94,** 742–759.
4. Suhrmann, R. & Mittmann, A. (1938) *Z. Phys.* **111,** 18–35.
5. Setton, R. & Bazin, J. (1962) *C. R. Hebd. Seances Acad. Sci.* **254,** 2150–2155.
6. Inokuchi, H. & Harada, Y. (1963) *Nature (London)* **198,** 477–478.
7. Ogino, K., Iwashima, S., Inokuchi, H. & Harada, Y. (1965) *Bull. Chem. Soc. Jpn.* **38,** 473–477.
8. Marchetti, A. & Kearns, D. R. (1966) *J. Chem. Phys.* **44,** 1301–1302.
9. Aleksandrov, V. V. & Belkind, A. I. (1975) *Latv. PSR Zinat. Akad. Vestis Fiz. Teh. Zinat. Ser. (2),* 30–40.
10. Belkind, A. I. (1979) *Photoemission from Organic Solids* (Sinatne, Riga, U.S.S.R.), pp. 5–185.
11. Rossi-Fanelli, A. & Antonini, E. (1959) *Arch. Biochem. Biophys.* **80,** 299–307.
12. Birrell, G. B., Hedberg, K. K. & Griffith, O. H. (1987) *J. Histochem. Cytochem.* **35,** 843–853.
13. Sommer, A. H. (1968) *Photoemissive Materials* (Wiley, New York), pp. 1–174.
14. Massey, G. A & Imthurn, G. P. (1988) *IEEE J. Quantum Electron.* **24,** 703–705.
15. Berthold, D. A, Babcock, G. T. & Yocum, C. F. (1981) *FEBS Lett.* **134,** 231–234.
16. Thompson, J. C. (1976) *Electrons in Liquid Ammonia* (Clarendon, Oxford), p. 2.
17. Dye, J. L. (1987) *Sci. Am.* **257** (3), 66–75.
18. Huang, R. H., Ward, D. L., Kuchenmeister, M.E. & Dye, J. L. (1987) *J. Am. Chem. Soc.* **109,** 5561–5563.
19. Boschi, R., Clar, E. & Schmidt, W. (1974) *J. Chem. Phys.* **60,** 4406–4418.
20. Gutmann, F. & Lyons, L. E. (1967) *Organic Semiconductors* (Wiley, New York), pp. 693–694.
21. Schechtman, B. H. (1968) Ph.D. Thesis (Stanford Univ., Stanford, CA), p. 206.
22. Nakahara, H., Fukuda, K. & Inokuchi, H. (1979) *Chem. Lett.* **5,** 453–456.
23. Paul, D. E., Lipkin, D. & Weissman, S. I. (1956) *J. Am. Chem. Soc.* **78,** 116–120.
24. McConnell, H. M. & Chesnut, D. B. (1958) *J. Chem. Phys.* **28,** 107–117.
25. Wertz, J. E. & Bolton, J. R. (1972) *Electron Spin Resonance* (McGraw-Hill, New York), Chapts. 5–6.
26. Fujita, I., Davis, M. S. & Fajer, J. (1978) *J. Am. Chem. Soc.* **100,** 6280–6282.
27. Mauzerall, D. & Feher, G. (1964) *Biochim. Biophys. Acta* **79,** 430–432.